Role of Buried Polar Residues in Helix Bundle Stability and Lipid Binding of Apolipophorin III: Destabilization by Threonine 31[†]

Paul M. M. Weers,* Wazir E. Abdullahi, Jamie M. Cabrera, and Tzu-Chi Hsu

Department of Chemistry and Biochemistry, California State University at Long Beach, Long Beach, California 90840

Received March 18, 2005; Revised Manuscript Received May 2, 2005

ABSTRACT: Apolipophorin III (apoLp-III) from *Locusta migratoria* is a model exchangeable apolipoprotein that plays a key role in neutral lipid transport. The protein is comprised of a bundle of five amphipathic α-helices, with most hydrophobic residues buried in the protein interior. The low stability of apoLp-III is thought to be crucial for lipid-induced helix bundle opening, to allow protein−lipid interactions. The presence of polar residues in the hydrophobic protein interior may facilitate this role. To test this, two buried polar residues, Thr-31 and Thr-144, were changed into alanine by site-directed mutagenesis. Secondary structure analysis and GdnHCl- and temperature-induced denaturation studies indicated an increase in α-helical content and protein stability for T31A apoLp-III compared to wild-type apoLp-III. In contrast, T144A had a decreased α-helical content and protein stability, while tryptophan fluorescence indicated increased exposure of the hydrophobic interior to buffer. Two mutant proteins that had lysine residues introduced in the hydrophobic core displayed a more pronounced decrease in secondary structure and protein stability. Lipid binding studies using phospholipid vesicles showed that T31A apoLp-III was able to transform phospholipid vesicles into discoidal particles but at a 3-fold reduced rate compared to wild-type apoLp-III. In contrast, the less stable apoLp-III mutants displayed an increased ability to transform phospholipid vesicles. These results demonstrate the inverse correlation between protein stability and the ability to transform phospholipid vesicles into discoidal protein−lipid complexes and that Thr-31 is a key determinant of the relatively low protein stability, thereby promoting apoLp-III to interact with lipid surfaces.

Lipoproteins are the vehicles for transport of hydrophobic material in plasma. These large complexes of lipids and proteins exchange lipids with various tissues. While structural apolipoproteins comprise the protein part of lipoproteins, additional exchangeable apolipoproteins can be found on the particle surface, e.g., apolipoprotein (apo)[1] E and A-I and apolipophorin III (apoLp-III). Functions of exchangeable apolipoproteins include maintenance of lipoprotein structural integrity, receptor binding, and enzyme regulation (*1*−*3*). Exchangeable apolipoproteins associate with lipoprotein surfaces through amphipathic α-helices (*4*). A lipid-induced conformational change facilitates interaction of the buried nonpolar face of the amphipathic helix with the new lipid environment, leading to a stable lipid-protein binding interaction. ApoLp-III (∼164 residues, ∼18 kDa) is a well-characterized apolipoprotein found in some insects (*5*). It has served well as a model exchangeable apolipoprotein to gain insight into the apolipoprotein structure−function relationship (*6*). NMR and X-ray structures of the protein in the lipid-free state are available for two different apoLp-IIIs, i.e., *Locusta migratoria* and *Manduca sexta* (*7*−*9*). Several studies led to important insight into the lipid-bound conformation of apoLp-III, and recent pyrene fluorescence and fluorescence resonance energy transfer measurements led to a new model for the protein in a lipid-bound state (*10*, *11*). This model of lipid-bound apoLp-III is remarkably similar to that of other models proposed for apoA-I and apoE (*12*−*17*). ApoLp-III is highly soluble in buffer and present as a monomer (*18*, *19*). X-ray and NMR solution structures revealed a protein comprised of a bundle of five amphipathic α-helices with a simple up-and-down topology (*7*, *8*). The majority of hydrophobic residues are buried in the protein interior while hydrophilic residues are located on the protein surface. This molecular architecture ensures a high protein solubility and bearing the propensity to switch to a lipid-bound conformation. To engage in lipid interaction, the hydrophobic face of the amphipathic helices become available by helix rearrangements, allowing direct lipid−protein contacts. This helix bundle opening is reversible, as lipid depletion leads to dissociation of apoLp-III from the lipoprotein surface and recovery of the helix bundle structure (*20*). Compared to other globular proteins, the stability of *M. sexta* and *L. migratoria* apoLp-III is noticeably low (ΔG 2.0−2.5 kcal mol^{-1}, midpoints of GdnHCl denaturation vary between 0.3 and 0.6 M) (*18*, *19*, *21*, *22*). It has been suggested that low apolipoprotein stability mediates the lipid-induced conformational change, allowing the formation of a stable lipid−protein complex (*8*, *9*). It was noticed that the protein contains several hydrophilic residues buried in the hydrophobic interior. These residues have been hypothesized to play an important role in destabilizing the helix

[†] This work was supported by National Institutes of Health Grant HL 077135.

* Address correspondence to this author. Tel: 562-985-4948. Fax: 562-985-8557. E-mail: pweers@csulb.edu.

[1] Abbreviations: apo, apolipoprotein; apoLp-III, apolipophorin III; DMPC, dimyristoylphosphatidylcholine; ANS, 8-anilino-1-naphthalenesulfonate; LDL, low-density lipoprotein; PBS, phosphate-buffered saline.

10.1021/bi050502v CCC: $30.25
Published on Web 05/27/2005

bundle structure of apoLp-III and promoting lipid-induced helix rearrangements. Earlier studies also indicated an important role for helix 1 and helix 5 in the initial lipid and lipoprotein binding in *L. migratoria* apoLp-III (*23*). We have addressed the role of polar residues in the hydrophobic interior by using site-directed mutagenesis to introduce changes in the hydrophobic interior of *L. migratoria* apoLp-III. Two threonine residues that reside in helix 1 and helix 5 were changed into alanine, and their effect on secondary structure, protein stability, and lipid interaction was analyzed. Conversely, positively charged side chains were introduced in the hydrophobic face of helix 1 and helix 5 to cause disturbances in the hydrophobic helix bundle interior. In the present study we have found that Thr-31 plays an important role in lowering helix bundle stability, thereby promoting lipid binding interaction.

EXPERIMENTAL PROCEDURES

Protein Expression and Site-Directed Mutagenesis. ApoLp-III was expressed in 1 L *Escherichia coli* BL21(DE3) cultures as previously reported in detail (*24*). The purification of the protein samples was verified by sodium dodecyl sulfate−polyacrylamide gel electrophoresis (Novex Tris−glycine 4−20% gradient gels; Invitrogen Co., Carlsbad, CA). Site-directed mutagenesis was carried out by the QuickChange II site-directed mutagenesis kit according to the manufacturer's instructions (Stratagene, La Jolla, CA), using 25 ng of template DNA and 12−16 cycles. The following primer pairs were employed (MWG Biotech, High Point, NC): L17K, 5′-GGCGGTGCAGCAGAAGAACCACACCATCGT-3′ and 5′-GACGATGGTGTGGTTCTTCTGCTGCACCGCC-3′; A140K, 5′-GCGCGCTGCAGGAGAAGGCCGAGAAGACCAAGG-3′ and 5′-CCTTGGTCTTCTCGGCCTTCTCCTGCAGCGCGC-3′; T31A, 5′-GCTGCACGAGGCTCTGGGCCTGC-3′ and 5′-GCAGGCCCAGAGCCTCGTGCAGC-3′; T144A, 5′-CCGCCGAGAAGGCCAAGGAGGCAGC-3′ and 5′-GCTGCCTCCTTGGCCTTCTCGGCGG-3′. DNA sequence analysis of both strands was carried out at the CSUPERB Microchemical Core Facility DNA Lab at California State University, San Diego.

Circular Dichroism. ApoLp-III samples (0.2 mg/mL in 50 mM sodium phosphate, pH 7.4) were analyzed in a Jasco 810 spectropolarimeter, and scans were obtained between 185 and 260 nm (average of three scans). Denaturation studies were performed in phosphate-buffered saline (PBS; 127 mM NaCl, 2.7 mM KCl, 10 mM Na_2HPO_4, 2 mM KH_2PO_4, pH 7.4). ApoLp-III samples (0.4 mg/mL) were incubated in the presence of GdnHCl for 16 h, and ellipticity was measured at 222 nm. Temperature-induced denaturation was carried out between 30 and 80 °C, using an increase of 5 °C min^{-1}, in a Jasco Peltier temperature control unit (model 4235). The α-helical content was calculated using the self-consistent method using Dicroprot version 2.6 (*25*). The free energy of unfolding was calculated using the following equation assuming a two-state mechanism according to Pace (*26*):

$$K_D = e^{-\Delta G_D/RT}$$

K_D was calculated from the fraction of denatured protein (f_D)/fraction of native protein (f_N) obtained from the GdnHCl denaturation curves expressed as percent maximal change, assuming $f_N + f_D = 1$. Extrapolation of ΔG_D versus GdnHCl concentration yielded the free energy change of unfolding in the absence of GdnHCl, $\Delta G_D^{H_2O}$.

Fluorescence. Fluorescence studies were carried out in a Fluormax-2 fluorescence spectrometer. ApoLp-III tryptophan residues were excited at 280 nm with emission monitored between 290 and 450 nm (excitation/emission slit width 5 nm) using a protein concentration of 0.1 mg/mL PBS. The wavelength of the tryptophan fluorescence emission maximum (λ_{max}) was the average of three determinations (±1 nm). Experiments with 8-anilinonaphthalene-1-sulfonate (ANS; Sigma Co., St. Louis, MO) were carried out in PBS at 5.6 μM apoLp-III and 250 μM ANS concentration. ANS fluorescence was measured in the absence and presence of apoLp-III, and samples were excited at 395 nm with emission monitored between 400 and 550 nm (excitation/emission slit width 5 nm).

Phospholipid Vesicle Clearance. Dimyristoylphosphatidylcholine (DMPC; Avanti Polar Lipids, Birmingham, AL) was dissolved in PBS, incubated for 2 min at 37 °C, and vigorously vortexed for 1 min. ApoLp-III and DMPC dispersions were mixed at a protein:lipid weight ratio of 2:1 and incubated in a 1 mL cuvette in a Shimadzu 2401 spectrophotometer while a temperature of 23.9 °C was maintained using a Peltier temperature-controlled cuvette holder (TCC-240A). Formation of lipid−protein complexes was monitored spectrophotometrically at 325 nm for 15 min, and first-order rate constants (k) were calculated from the decrease in sample absorbance. In the absence of apoLp-III, DMPC vesicle dispersions did not show a decrease in absorbance during the 15 min incubation period.

Lipoprotein Binding. The ability of apoLp-III to bind to spherical lipoproteins was studied using human LDL. Treatment of LDL with phospholipase C promotes the formation of diacylglycerol on the lipoprotein surface, thereby promoting formation of LDL aggregates. ApoLp-III affords protection against aggregation via association with the lipoprotein surface (*27*). LDL (50 μg of protein; Intracel, Frederick, MD) was incubated with 160 milliunits of phospholipase C from *Bacillus cereus* (Sigma Co., St. Louis, MO) in the absence or presence of 50 μg of T31A, T144A, T31A/T144A, L17K, A140K, or wild-type apoLp-III in buffer (50 mM Tris-HCl, 150 mM NaCl, 2 mM $CaCl_2$, pH 7.5). To monitor formation of LDL aggregates, the absorbance was measured in a Multiskan Ascent plate reader (Thermo Labsystems, Helsinki, Finland) at 340 nm at the times indicated. All measurements were done in triplicate.

RESULTS

Design of Mutant Proteins. There are 22 buried or partially buried hydrophilic residues present in *L. migratoria* apoLp-III that may cause the protein's marginal stability (*9*). We focused our study on residues located in helix 1 and helix 5 as both helices have been implied in initial lipid binding interaction (*23*). Two hydrophilic residues were selected: Thr-31 and Thr-144. Both residues are located between helix 1 and helix 5 and are considered to be buried as their fractional solvent-accessible surface areas are 0.00 and 0.06, respectively (*9*). The location of these residues in the helix bundle interior is depicted in Figure 1. Both threonine residues were thought to be key residues to partially

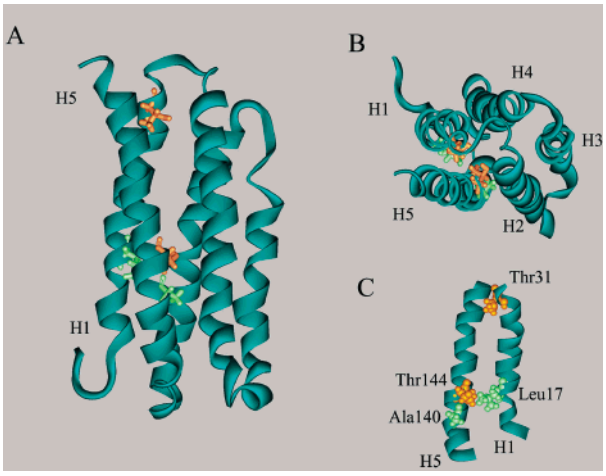

FIGURE 1: High-resolution structures of *L. migratoria* apoLp-III. Panel A shows a side view of apoLp-III with Thr-31 and Thr-144 (orange) and Leu-17 and Ala-140 (green). Panel B is an end-on view from the top of the protein, while panel C shows the location of the mutated residues seen from the center of the protein. The structure is based on the NMR solution structure, PDB code 1LS4 (*9*).

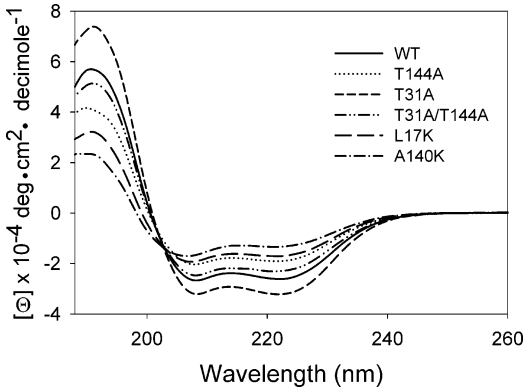

FIGURE 2: Secondary structure analysis of mutant apoLp-III. The ellipticity of mutant apoLp-IIIs (0.2 mg/mL in 50 mM sodium phosphate, pH 7.2) was measured by circular dichroism between 185 and 260 nm and compared to wild-type (WT) protein (solid line).

destabilize the helix bundle protein. By site-directed mutagenesis the threonine residues were mutated into alanine, individually or together. Furthermore, two fully buried hydrophobic residues were mutated into lysine residues. The introduction of positive charges in the helix bundle interior was intended to create disturbances in the helix bundle interior to study their effect on protein structure and lipid binding. The following mutant proteins were designed and expressed in *E. coli*: T31A, T144A, T31A/T144A, L17K, and A140K apoLp-III.

Circular Dichroism. The mutant proteins were analyzed by circular dichroism for secondary structure content and compared to wild-type apoLp-III. Circular dichroism scans between 190 and 260 nm showed the two troughs at 208 and 222 nm, indicating that the mutant proteins were α-helical. Nevertheless, differences between the various spectra were observed (Figure 2). Secondary structure calculations revealed a decrease in α-helical content and a corresponding increase in turns and unordered structure for all mutants except T31A apoLp-III. L17K and A140K apoLp-III displayed a strong decrease in α-helical content,

Table 1: Biophysical Properties of Mutant ApoLp-III[a]

apoLp-III	$\Delta G_D^{H_2O}$ (kcal/mol)	Gdn-HCl$_{1/2}$ (M)	$T_{1/2}$ (°C)	α-helix (%)	Trp λ_{max} (nm)	ANS (487 nm)
WT	2.05	0.51	53	73	338	1.0
T31A	2.65	0.62	57	89	337	0.9
T144A	0.73	0.28	44	58	342	1.4
T31A/ T144A	0.99	0.37	46	67	341	1.8
L17K	0.69	0.20	37	48	344	1.1
A140K	0.36	0.16	38	41	347	1.0

[a] $\Delta G_D^{H_2O}$ is the free energy of unfolding in the absence of GdnHCl; the midpoint of GdnHCl denaturation (GdnHCl$_{1/2}$) and temperature denaturation ($T_{1/2}$) was obtained from molar ellipticity measurements at 222 nm. The amount of α-helix was calculated using the self-consistent method (*25*). The tryptophan maximum emission wavelength (λ_{max}) was obtained from emission scans of apoLp-III samples excited at 280 nm. ANS values are the ratios to wild-type apoLp-III (excitation at 395 nm, emission intensity measured at 487 nm).

and also T144A and T31A/T144A apoLp-III displayed a reduction in helical content (values ranging from 41% to 73%; see Table 1). In contrast, the helical content for T31A apoLp-III was considerably larger compared to wild-type apoLp-III. This may indicate an important structural role of Thr-31.

Fluorescence. To further probe for changes in protein structure, intrinsic tryptophan fluorescence studies were performed. *L. migratoria* apoLp-III bears two tryptophan residues, Trp-115 and Trp-130, which are completely and partially buried, respectively. These tryptophan residues have been shown to be sensitive to environmental changes, responding to exposure to buffer or lipid by increases or decreases in their emission wavelength maximum (*28*, *29*). Analysis of the tryptophan emission spectra (not shown) revealed that λ_{max} of T31A apoLp-III was essentially similar to that of wild-type apoLp-III (Table 1). However, the other mutations caused a considerable increase in λ_{max}, indicative of increased exposure to buffer. The increase was highest for both mutants with lysine residues in the hydrophobic face of their helices. The observed increase in λ_{max} indicated that these tryptophan residues became partially exposed to the hydrophilic milieu, possibly a result of local disturbances in the helix bundle structure caused by the amino acid substitutions.

Secondly, ANS fluorescence was used to probe for exposed hydrophobic surface as a result of the amino acid substitutions. As demonstrated in previous studies (*29*), ANS fluorescence intensity (excitation 395 nm) of mixtures of wild-type apoLp-III in the presence of excess ANS was relatively low, but with a pronounced shift from ~520 nm to 487 nm. Fluorescence intensity emission was essentially similar for T31A apoLp-III, in contrast with T144A and T31A/T144A apoLp-III, which showed increased ANS fluorescence intensity (Figure 3). Thus, tryptophan and ANS fluorescence measurements indicate increased exposure to buffer and increase in exposed hydrophobic pockets of T144A and T31A/T144A apoLp-III. When lysine was introduced in the nonpolar face of helix 1 or helix 5, ANS fluorescence intensity did not change compared to wild-type apoLp-III (Table 1). This may be explained by a low secondary structure content of both L17K and A140K mutant proteins, containing few exposed hydrophobic pockets in the hydrophobic faces of their α-helices.

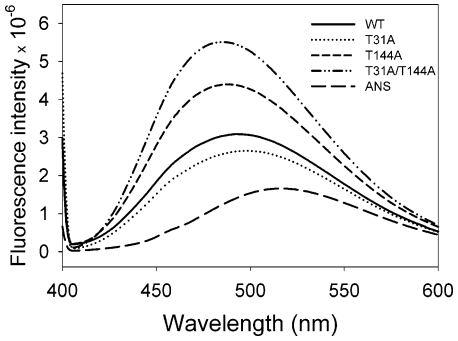

FIGURE 3: ANS fluorescence. ApoLp-III was mixed with an excess of the hydrophobic dye ANS and excited at 395 nm, and emission was monitored between 400 and 600 nm.

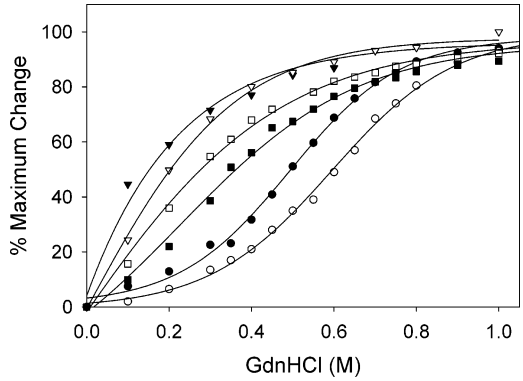

FIGURE 4: GdnHCl denaturation of mutant apoLp-III. ApoLp-III was incubated with increasing amounts of GdnHCl and the ellipticity measured at 222 nm: wild-type (closed circles), T31A (open circles), T144A (open squares), T31A/T144A (closed squares), L17K (open triangles), and A140K (closed triangles).

GdnHCl and Temperature Denaturation. Protein stability studies were carried out by circular dichroism. Protein samples were denatured with increasing amounts of GdnHCl, and the decrease in molar ellipticity was measured at 222 nm. The denaturation curves showed that T31A apoLp-III had a significant increased resistance to GdnHCl-induced denaturation (Figure 4), as indicated by the increase from 0.51 M (wild-type apoLp-III) to 0.62 M GdnHCl (T31A apoLp-III). On the other hand, T144A and T31A/T144A apoLp-III showed decreased resistance to GdnHCl denaturation. The mutants with alanine or leucine to lysine substitutions displayed a strong decrease in the midpoint of GdnHCl denaturation. Temperature denaturation curves were obtained between 30 and 80 °C, showing a decrease in ellipticity (222 nm) above 35 °C, until a temperature of 70 °C was reached, after which no further changes were observed (not shown). Upon cooling the ellipticity was regained, indicating complete reversal of the temperature-induced denaturation, in good agreement with previous studies (*18*, *30*). As depicted in Table 1, T31A apoLp-III displayed the highest midpoint of temperature denaturation (57 °C), followed by wild-type (53 °C), T31A/T144A (46 °C), T144A (44 °C), A140K (38 °C), and L17K (37 °C). This decreasing order of resistance to temperature denaturation is similar to that of GdnHCl-induced denaturation. The free energy change of apoLp-III unfolding was determined from the GdnHCl denaturation curves (*26*). For wild-type apoLp-III, a $\Delta G_D^{H_2O}$ of 2.1 kcal mol^{-1} was calculated, while a value of 2.7 kcal mol^{-1} was obtained for T31A apoLp-III. As expected, the other mutants

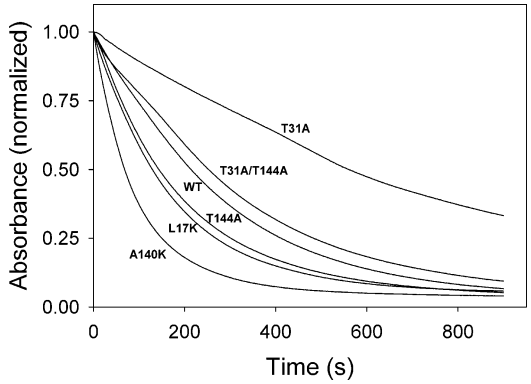

FIGURE 5: DMPC vesicle clearance. Multilamellar DMPC vesicles were incubated in the presence of apoLp-III at the lipid transition temperature using a protein to lipid mass ratio of 2:1. In the absence of apoLp-III, the suspension remains turbid (not shown), while in the presence of apoLp-III, the vesicles are rapidly transformed into much smaller discoidal complexes, as indicated by the decrease in sample absorbance (measured at 325 nm).

showed significantly reduced $\Delta G_D^{H_2O}$ values, with both lysine mutants showing the lowest free energy of unfolding.

Phospholipid Vesicle Clearance. To test the ability of the apoLp-III mutants to interact with phospholipid vesicles, the apolipoproteins were incubated in the presence of multilamellar DMPC vesicles near the gel−liquid-crystalline phase transition temperature (23.9 °C). At this temperature the large phospholipid vesicles are transformed into small discoidal particles, having a diameter of approximately 19 nm based on electron microscopy measurements (*29*). Since vesicle dispersions have a turbid appearance while solutions of small discoidal lipoproteins are optically clear, the transformation of vesicles into disks can be monitored by measurement of the apparent absorbance at 325 nm. As shown in Figure 5, incubation of wild-type apoLp-III with the DMPC vesicle dispersion caused a rapid decrease in sample absorbance, indicative of the formation of discoidal protein−lipid particles (solid line, first-order rate constant $k = 3.3 \times 10^{-3}$ s^{-1}). On the other hand, the ability of the more stable T31A mutant to cause vesicle transformation was greatly hampered, having a 3-fold reduced rate ($k = 1.2 \times 10^{-3}$ s^{-1}). While wild-type apoLp-III completely transformed the vesicles into disks during the incubation period, the T31A apoLp-III-induced clearance was not complete as the sample remained partially turbid (∼35% of maximum). The mutants that had lower protein stability properties all displayed enhanced transformation rates as indicated by their rate constants: L17K, $k = 4.7 \times 10^{-3}$ s^{-1}; A140K, $k = 7.8 \times 10^{-3}$ s^{-1}; T144A, $k = 4.3 \times 10^{-3}$ s^{-1}; T31A/T144A, $k = 2.8 \times 10^{-3}$ s^{-1}.

Lipoprotein Binding. Previous studies with apoLp-III have shown substantial differences between liposome clearance and lipoprotein binding (*30*, *31*). In view of the large increase in phospholipid vesicle transformation rates of both low structure lysine mutants, an additional assay was used to test if these mutant proteins retained their ability to bind to spherical lipoprotein surfaces. This was carried out using human LDL. When human LDL is treated with phospholipase C, diacylglycerol appears on the lipoprotein surface. These hydrophobic defects cause LDL to aggregate, as evident by the increase in sample absorbance at 340 nm. The presence of apoA-I, apoE, or apoLp-III in phospholipase

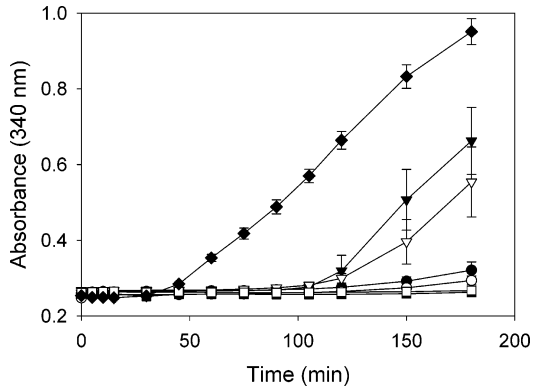

FIGURE 6: LDL aggregation protection assay. Phospholipase C treated LDL was incubated in the absence (closed diamonds) or presence of various apoLp-III samples: wild-type (closed circles), T31A (open circles), T144A (open squares), T31A/T144A (closed squares), L17K (open triangles), and A140K (closed triangles). LDL aggregation, caused by enzymatic removal of the phosphatidylcholine headgroup by phospholipase C, is apparent by the increase in sample turbidity measured in a spectrophotometer at 340 nm ($n = 3$, mean ± SD).

C treated LDL samples prevents LDL aggregation through association of the apolipoproteins with the lipoprotein surface as demonstrated earlier (*27*). This protective role of apolipoproteins has been used previously to assay apoLp-III mutants for their ability to bind to the lipoprotein surface (*30*, *32*−*33*). This assay is especially valuable since the main function of apoLp-III in vivo is to associate with diacylglycerol-enriched lipoproteins (*20*). As shown in Figure 6, the absorbance of LDL increased rapidly in the presence of phospholipase C after an initial lag phase of 30 min, indicative of LDL aggregate formation. In contrast, when LDL was incubated simultaneously with wild-type, T31A, T144A, or T31A/T144A apoLp-III, increase in sample absorbance was prevented. This indicates that the apolipoproteins were able to bind to lipolyzed LDL, thereby affording protection against phospholipase C induced aggregation. Apparently, the threonine to alanine mutations did not affect the ability to associate with a lipoprotein surface. However, both L17K and A140K apoLp-III mutants were not able to prevent LDL from aggregation, as indicated by elevated absorbance levels after a 100 min incubation period.

DISCUSSION

ApoLp-III lipid binding is a complex process that involves recognition of hydrophobic defects, superficial binding, and helix rearrangement to form a stable lipid−protein complex. Previous studies indicated that a six-residue α-helix located between helix 3 and helix 4 in *M. sexta* apoLp-III plays a crucial role in initial lipid binding, thereby acting as a hydrophobic sensor (*33*). In *L. migratoria* apoLp-III, three leucine residues present in loops were identified to function in a similar role (*30*), while others suggested that a four-residue minihelix (residing in the loop connecting helix 4 and helix 5) was responsible for this role (*9*).

In the present study, the role of hydrophilic residues in the hydrophobic interior of the model exchangeable apolipoprotein apoLp-III was investigated. Structural examination of the protein's hydrophobic core led to the hypothesis that hydrophilic residues in the interior play a role in the marginal stability of apoLp-III as discussed by Wang and co-workers (*8*, *9*). It is hypothesized that the marginal stability of apoLp-III promotes the reversible interaction with lipoproteins as apoLp-III associates with or dissociates from lipoprotein surfaces in response to lipid changes on the lipoprotein surface. Such a marginal stability would facilitate helix bundle opening and allows interaction of buried hydrophobic residues with the lipid surface when helix−helix interactions are replaced by helix−lipid interactions. To form a stable lipid−protein complex, apoLp-III undergoes a large conformational change. Experiments with model phospholipid membranes have shown that the five-helix bundle protein switches to a large elongated α-helix, circumscribing the discoidal bilayer. Two molecules of apoLp-III are oriented side by side in an antiparallel orientation (*10*, *11*). Similar conformations have also been proposed for human apoE and apoA-I in discoidal particles (*12*−*17*, *34*). In addition, conformational flexibility ensures that apoLp-III can associate with discoidal lipoprotein particles with various sizes, and alternative conformations on spherical lipoprotein surfaces are likely.

In the present study, we have shown that Thr-31 is a key residue that destabilizes apoLp-III. Interestingly, Thr-31 flanks Leu-32 and Leu-34, residues that have been implicated in initiation of lipid binding (*30*). Substituting Thr-31 for alanine caused an increase in protein stability as indicated by a larger midpoint of GdnHCl and temperature denaturation and the free energy of unfolding in the absence of GdnHCl ($\Delta G_D^{H_2O}$). The effect of the mutations on lipid binding was measured by interaction with standard phospholipid vesicles made of DMPC. In support of our hypothesis about the role of threonine in the helix bundle interior, it was observed that T31A apoLp-III had a significantly reduced ability to transform DMPC vesicles into discoidal structures compared to the wild-type protein. This result is in good agreement with previous studies indicating that the stability of apolipoproteins is inversely correlated with protein stability as reported for apoE isoforms and their ability to clear liposome dispersions (*35*−*37*). ApoE is comprised of two independently folded domains (*38*, *39*), of which the N-terminal domain bears a striking similarity with apoLp-III (*40*). Moreover, the more stable N-terminal domain of apoE has a lower vesicle clearance capability compared to the less stable C-terminal domain of apoE (*36*). Also, induction of a loosely folded apolipoprotein favors lipid interaction. Such a molten globule retains its secondary structure but has limited tertiary contacts as indicated by increased ANS binding and exposure of tryptophan, suggesting a partially exposed hydrophobic interior. Evidence for a pH-induced molten globule has been found for two different apoLp-IIIs (*M. sexta* and *L. migratoria*) and the N-terminal domain of apoE. The loosely folded helix bundles with increased exposure of their hydrophobic interior were able to transform phospholipid vesicles with rates of an order of magnitude greater compared to the protein at neutral pH (*29*, *41*−*42*).

While Thr-144 was another residue thought to function in destabilizing the apoLp-III helix bundle, our study does not support this. In contrast, substitution of Thr-144 by alanine resulted in a decrease in protein stability as indicated by a lower midpoint of GdnHCl and temperature denaturation and $\Delta G_D^{H_2O}$. Also, T144A apoLp-III was able to transform phospholipid vesicles at a faster rate. The double mutant (T31A/T144A) displayed stability properties between wild-

type and T144A apoLp-III. Thus, the T144A induced instability was partly compensated by the T31A mutation. In apoLp-III there are 22 (*L. migratoria*) or 27 (*M. sexta*) polar or ionizable amino acid side chains in the core or helix interface (*8*, *9*). It is unlikely that each of these residues induces a low protein stability, and we found no evidence that Thr-144 was involved in this role.

As expected, substitution of Leu-17 and Ala-140 by lysine residues resulted in major changes in protein structure and stability, i.e., loss of α-helical structure, increased exposure of its hydrophobic interior to buffer, and less resistance to GdnHCl- and temperature-induced denaturation. In contrast to the enhanced interaction with phospholipid vesicles, the ability of the lysine mutants to interact with lipoprotein surfaces was strongly decreased, as they were not able to afford protection against phospholipase C induced aggregation of human LDL. It is evident that the positive charge at the hydrophobic face of the amphipathic helix not only caused challenges for proper protein folding but also hampered lipoprotein binding. Evidently, a properly folded protein is necessary for lipoprotein binding but may not be critical for phospholipid vesicle interaction as the lysine mutants displayed 2-fold higher phospholipid vesicle transformation rates compared to wild-type apoLp-III. This result is similar to studies with truncated forms of *Galleria mellonella* apoLp-III in which complete helices were removed. *G. mellonella* apoLp-III is an apolipoprotein very similar to *M. sexta* apoLp-III (*43*) and received considerable interest for its role in innate immunity (*44*−*46*). Removal of two helices resulted in a decrease in secondary structure and hampered lipoprotein binding but increased its ability to transform phospholipid vesicles into discoidal complexes (*22*). A better accessibility of the phospholipid bilayer to the hydrophobic interior of the less stable three-helix truncated proteins may have promoted helix bundle opening of the protein. Nevertheless, such major structural changes were unfavorable for lipoprotein surface interaction, and the lysine mutants of the present study are in good agreement with this observation.

Using the detailed structural knowledge of apoLp-III, we were able to design mutant proteins to test the stability hypothesis of the role of hydrophilic residues located in the protein core. Structural and functional characterization of five mutant apoLp-IIIs strongly suggests that Thr-31 promotes helix bundle instability and lipid binding. This study confirms the concept that the relatively low stability of apolipoproteins is important for its ability to interact with lipid surfaces through helix rearrangement. This study also supports the thought that differences in helix bundle stability can cause a major effect on apolipoprotein function, as seen in the apoE2, apoE3, and apoE4 isoforms (*35*, *47*). ApoLp-III is well suited for such studies because of the availability of X-ray and NMR solution structures of *L. migratoria* apoLp-III (*7*, *9*) and the NMR solution structure of *M. sexta* apoLp-III (*8*). Therefore, structural studies of apoLp-III will likely improve our understanding of apolipoprotein function.

ACKNOWLEDGMENT

We thank Drs. Vasanthy Narayanaswami and Vincent Raussens for comments on the manuscript.

REFERENCES

1. Weisgraber, K. H. (1994) Apolipoprotein E: structure function relationships, *Adv. Protein Chem. 45*, 249−302.
2. Marcel, Y. L., and Kiss, R. S. (2003) structure function relationships of apolipoprotein A-I: a flexible protein with dynamic lipid associations, *Curr. Opin. Lipidol. 14*, 151−157.
3. Saito, H., Lund-Katz, S., and Phillips, M. C. (2004) Contributions of domain structure and lipid interaction to the functionality of exchangeable human apolipoproteins, *Prog. Lipid Res. 43*, 350−380.
4. Segrest, J. P., Jones, M. K., De Loof, H., Brouillette, C. G., Venkatachalapathi, Y. V., and Anantharamaiah, G. M. (1992) The amphipathic helix in the exchangeable apolipoproteins: a review of secondary structure and function, *J. Lipid Res. 33*, 141−166.
5. Weers, P. M. M., and Ryan, R. O. (2003) Apolipophorin III: a lipid-triggered molecular switch, *Insect Biochem. Mol. Biol. 33*, 1249−1260.
6. Narayanaswami, V., and Ryan, R. O. (2000) Molecular basis of exchangeable apolipoprotein function, *Biochim. Biophys Acta 1483*, 15−36.
7. Breiter, D. R., Kanost, M. R., Benning, M. M., Wesenberg, G., Law, J. H., Wells, M. A., Rayment, I., and Holden, H. M. (1991) Molecular structure of an apolipoprotein determined at 2.5-Å resolution, *Biochemistry 30*, 603−608.
8. Wang, J., Sykes, B. D., and Ryan, R. O. (2002) Structural basis for the conformational adaptability of apolipophorin III, a helix bundle exchangeable apolipoprotein, *Proc. Natl. Acad. Sci. U.S.A. 99*, 1188−1193.
9. Fan, D., Zheng, Y., Yang, D., and Wang, J. (2003) NMR solution structure and dynamics of an exchangeable apolipoprotein, *Locusta migratoria* apolipophorin III, *J. Biol. Chem. 278*, 21212−21220.
10. Garda, H. A., Arrese, E. L., and Soulages, J. L. (2002) Structure of apolipophorin III in discoidal lipoproteins. Interhelical distances in the lipid-bound state and conformational change upon binding to lipid, *J. Biol. Chem. 277*, 19773−19782.
11. Sahoo, D., Weers, P. M. M., Ryan, R. O., and Narayanaswami, V. (2002) Lipid triggered molecular switch of apoLp-III helix bundle to an extended helix conformation, *J. Mol. Biol. 321*, 201−214.
12. Koppakka, V., Silvestro, L., Engler, J. A., Brouillette, C. G., and Axelsen, P. H. (1999) The structure of human lipoprotein A-I. Evidence for the "belt" model, *J. Biol. Chem. 274*, 14541−14544.
13. Segrest, J. P., Jones, M. K., Klon, A. E., Sheldahl, C. J., Hellinger, M., De Loof, H., and Harvey, S. C. (1999) A detailed molecular belt model for apolipoprotein A-I in discoidal high-density lipoprotein, *J. Biol. Chem. 274*, 31755−31758.
14. Fisher, C. A., Narayanaswami, V., and Ryan, R. O. (2000) The lipid associated conformation of the receptor binding domain of human apolipoprotein E, *J. Biol. Chem. 275*, 33601−33606.
15. Li, H., Lyles, D. S., Thomas, M. J., Pan, W., and Sorci-Thomas, M. G. (2000) Structural determination of lipid-bound apoA-I using fluorescence energy transfer, *J. Biol. Chem. 275*, 37048−37054.
16. Lu, B., Morrow, J. A., and Weisgraber, K. H. (2000) Conformational reorganization of the four-helix bundle of human apolipoprotein E in binding to phospholipid, *J. Biol. Chem. 275*, 20775−20781.
17. Narayanaswami, V., Maiorano, J. N., Dhanasekaran, P., Ryan, R. O., Phillips, M. C., Lund-Katz, S., and Davidson, W. S. (2004) Helix orientation of the functional domains in apolipoprotein E in discoidal high-density lipoprotein particles, *J. Biol. Chem. 279*, 14273−14279.
18. Ryan, R. O., Oikawa, K., and Kay, C. M. (1993) Conformational, thermodynamic and stability properties of *Manduca sexta* apolipophorin III, *J. Biol. Chem. 268*, 1525−1530.
19. Weers, P. M. M., Kay, C. M., Oikawa, K., Wientzek, M., Van der Horst, D. J., and Ryan, R. O. (1994) Factors affecting the stability and conformation of *Locusta migratoria* apolipophorin III, *Biochemistry 33*, 3617−3624.
20. Van der Horst, D. J., Van Hoof, D., Van Marrewijk, W. J. A., and Rodenburg, K. W. (2002) Alternative lipid mobilization: the insect shuttle system, *Mol. Cell. Biochem. 239*, 113−119.
21. Narayanaswami, V., Yamauchi, Y., Weers, P. M. M., Maekawa, H., Sato, R., Tsuchida, K., Oikawa, K., Kay, C. M., and Ryan, R. O. (2000) Spectroscopic characterization of the conformational adaptability of *Bombyx* mori apolipophorin III, *Eur. J. Biochem. 267*, 728−736.
22. Dettloff, M., Niere, M., Ryan, R. O., Kay, C. M., Wiesner, A., and Weers, P. M. M. (2002) Differential lipid binding of truncation

mutants of *Galleria mellonella* apolipophorin III, *Biochemistry 41*, 9688−9695.
23. Soulages, J. L., Arrese, E. L., Chetty, P. S., and Rodriguez, V. (2001) Essential role of the conformational flexibility of helices 1 and 5 on the lipid binding activity of apolipophorin III, *J. Biol. Chem. 276*, 34162−34166.
24. Weers, P. M. M., Wang, J., Van der Horst, D. J., Kay, C. M., Sykes, B. D., and Ryan, R. O. (1998) Recombinant locust apolipophorin III: characterization and NMR spectroscopy, *Biochim. Biophys. Acta 1393*, 99−107.
25. Sreerama, N, and Woody, R. E. (1993) A self-consistent method for the analysis of protein secondary structure from circular dichroism, *Anal. Biochem. 209*, 32−44.
26. Pace, C. N. (1986) Determination and analysis of urea and guanidine hydrochloride denaturation curves, *Methods Enzymol. 131*, 266−279.
27. Liu, H., Scraba, D. G., and Ryan, R. O. (1993) Prevention of phospholipase-C induced aggregation of low-density lipoprotein by amphipathic apolipoproteins, *FEBS Lett. 316*, 27−33.
28. Weers, P. M. M., Prenner, E. J., Kay, C. M., and Ryan, R. O. (2000) Lipid binding of the exchangeable apolipoprotein apolipophorin III induces major changes in fluorescence properties of tryptophans 115 and 130, *Biochemistry 39*, 6874−6880.
29. Weers, P. M. M., Kay, C. M., and Ryan, R. O. (2001) Conformational changes of an exchangeable apolipoprotein, apolipophorin III from *Locusta migratoria*, at low pH: correlation with lipid binding, *Biochemistry 40*, 7754−7760.
30. Weers, P. M. M., Narayanaswami, V., Kay, C. M., and Ryan, R. O. (1999) Interaction of an exchangeable apolipoprotein with phospholipid vesicles and lipoprotein particles. Role of leucines 32, 34 and 95 in *Locusta migratoria* apolipophorin III, *J. Biol. Chem. 274*, 21804−21810.
31. Chetty, P. S., Arrese, E. L., Rodriguez, V., and Soulages, J. L. (2003) Role of helices and loops in the ability of apolipophorin-III to interact with native lipoproteins and form discoidal lipoprotein complexes, *Biochemistry 42*, 15061−15067.
32. Narayanaswami, V., Wang, J., Kay, C. M., Scraba, D. G., and Ryan, R. O. (1996) Disulfide bond engineering to monitor conformational opening of apolipophorin III during lipid binding, *J. Biol. Chem. 271*, 26855−26862.
33. Narayanaswami, V., Wang, J., Schieve, D., Kay, C. M., and Ryan, R. O. (1999) A molecular trigger of lipid-binding induced opening of a helix bundle exchangeable apolipoprotein, *Proc. Natl. Acad. Sci U.S.A. 96*, 4366−4371.
34. Borhani, D. W., Rogers, D. P., Engler, J. A., and Brouillette, C. G. (1997) Crystal structure of truncated human apolipoprotein A-I suggests a lipid-bound conformation, *Proc. Natl. Acad. Sci. U.S.A. 94*, 12291−12296.
35. Morrow, J. A., Hatters, D. M., Lu, B., Hochtl, P., Oberg, K. A., Rupp, B., and Weisgraber, K. H. (2002) Apolipoprotein E4 forms a molten globule. A potential basis for its association with disease, *J. Biol. Chem. 277*, 50380−55038.
36. Segall, M. L., Dhanasekaran, P., Baldwin, F., Anantharamaiah, G. M., Weisgraber, K. H., Phillips, M. C., and Lund-Katz, S. (2002) Influence of apoE domain structure and polymorphism on the kinetics of phospholipid vesicle solubilization, *J. Lipid Res. 43*, 1688−1700.
37. Weers, P. M. M., Narayanaswami, V., Choy, N., Luty, R., Hicks, L., Kay, C. M., and Ryan, R. O. (2003) Lipid binding ability of human apolipoprotein E N-terminal domain isoforms: correlation with protein stability?, *Biophys. Chem. 100*, 481−492.
38. Wetterau, J. R., Aggerbeck, L. P., Rall, S. C., Jr., and Weisgraber, K. H. (1988) Human apolipoprotein E3 in aqueous solution I. Evidence for two structural domains, *J. Biol. Chem. 263*, 6240−6248.
39. Aggerbeck, L. P., Wetterau, J. R., Weisgraber, K. H., Wu, C.-S. C., and Lindgren, F. T. (1988) Human apolipoprotein E3 in aqueous solution II. Properties of the amino- and carboxyl-terminal domains, *J. Biol. Chem. 263*, 6249−6258.
40. Wilson, C., Wardell, M. R., Weisgraber, K. H., Mahley, R. W., and Agard, D. A. (1991) Three-dimensional structure of the LDL receptor-binding domain of human apolipoprotein E, *Science 252*, 1817−1822.
41. Soulages, J. L., and Bendavid, O. J. (1998) The lipid binding activity of the exchangeable apolipoprotein apolipophorin-III correlates with the formation of a partially folded conformation, *Biochemistry 37*, 10203−10210.
42. Weers, P. M. M., Narayanaswami, V., and Ryan, R. O. (2001) Modulation of the lipid binding properties of the N-terminal domain of human apolipoprotein E3, *Eur. J. Biochem. 268*, 3728−3735.
43. Weise, C., Franke, P., Kopáček, P., and Wiesner, A. (1998) Primary structure of apolipophorin-III from the greater wax moth, *Galleria mellonella*, *J. Protein Chem. 17*, 633−641.
44. Wiesner, A., Losen, S., Kopáček, P., Weise, C., and Götz, P. (1997). Isolated apolipophorin III from *Galleria* mellonella stimulates the immune reactions of this insect, *J. Insect Physiol. 43*, 383−391.
45. Whitten, M. M. A., Tew, I. F., Lee, B. L., and Ratcliffe, N. A. (2004) A novel role for an insect apolipoprotein (apolipophorin III) in beta-1,3-glucan pattern recognition and cellular encapsulation reactions, *J. Immunol. 172*, 2177−2185.
46. Pratt, C. C., and Weers, P. M. M. (2004) Lipopolysaccharide binding of an exchangeable apolipoprotein, apolipophorin III, from *Galleria mellonella*, *Biol. Chem. 385*, 1113−1119.
47. Morrow, J. A., Segall, M. L., Lund-Katz, S., Phillips, M. C., Knapp, M., Rupp, B., and Weisgraber, K. H. (2000) Differences in stability among the human apolipoprotein E isoforms determined by the amino-terminal domain, *Biochemistry 39*, 11657−11666.

BI050502V